Notes for figure format in *Biomimetic Intelligence and Robotics*

- The width of figures in a **single column** should be **6-8 cm**, and the width of figures in the **full column** should be **12-17 cm**.
- The text in the figure (including the axis scale) should be **Arial font with 8 points**. The legend should be Arial font with 6 points.
- For figures with subfigures, use only "(a), (b), (c)…" in 9 points with Arial font for the figure captions, and place it in the middle below the subfigures.
- The thickness of line in figures (flowchart, coordinate and so on) is recommended to be 5 points in PS, or 0.75 pt in visio. Please make sure the maximum scale value of the axes in the graph covers the actual value.
- All figures should be of high resolution (600 dpi is necessary)
- Please provide figures in PDF, PNG, TIF, etc. JPG format is not recommended. And the Editable image source files in VISIO, PPT, PS, etc. are recommended to provide at the same time.

The size of figures can refer to the samples in the next page.

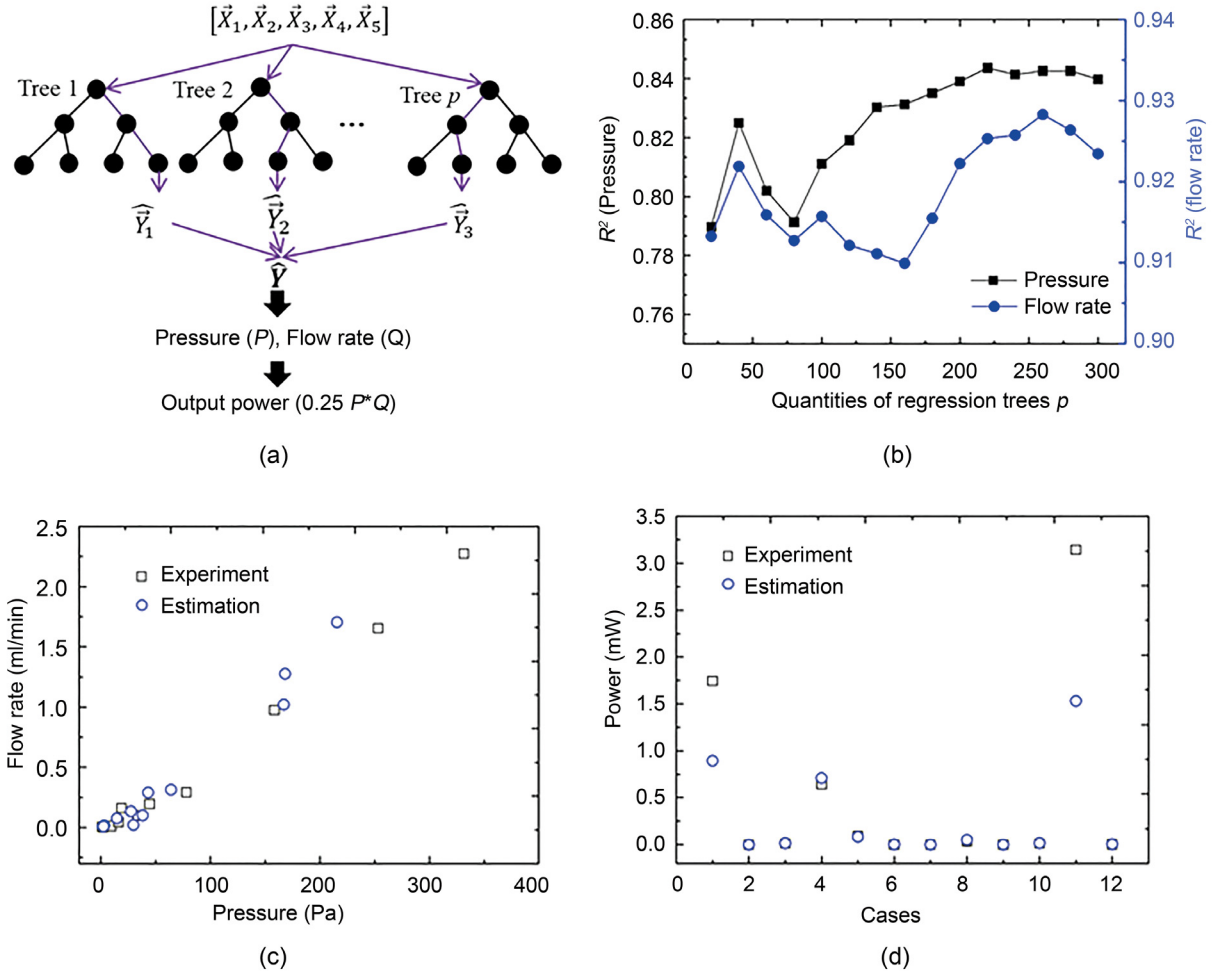

Fig. 3. (a) Random Forest regression algorithm. (b) Relation between the coefficient of determination (R^2) and quantities of regression trees relative to pressure and flow rate. (c) Comparison between the experimental and predicted values in terms of pressure and flow rate. (d) Experimental power and predicted power using the Random Forest regression algorithm.

seek the proportional relationship between the input and output variables. We employed the hyperbolic tangent function as an activation function of the hidden layer and the identity function for the output layer. Such two combination shows optimal accuracy after tuning our model with various kind of transfer function in the training process.

$$\text{Hidden layer: } \tanh(x) = \frac{2}{1+e^{-2x}} - 1 \tag{7}$$

$$\text{Output layer: } f(x) = x \tag{8}$$

Since the number of hidden layers is determined by a trial-and-error process, we adopted two hidden layers in our study. To optimize the model's weights in our study, MLP was set to incorporate the backpropagation algorithm with a stochastic gradient-based optimizer. By selecting the appropriate iteration, we trained the present model until the models converged completely. L regularization is used to prevent overfitting. The cost function of a linear regression model with L regularization:

$$Cost = L(\boldsymbol{w}, b) + \frac{\lambda}{2}\|\boldsymbol{w}\|^2 \tag{9}$$

where L denotes the loss function, $\boldsymbol{w}$, and b are the weight and bias parameters, respectively, and λ indicates a non-negative hyperparameter. Smaller λ correspond to less constrained $\boldsymbol{w}$, while larger λ more strongly constrained $\boldsymbol{w}$. This hyperparameter forces all coefficients to be close to zero but does not allow them to be equal to zero. Here, we adjust the hyper-parameter lambda (λ), ranging from 0 to 300, to seek the best predictor for the generated pressure and flow rate of EHD pumps (Fig. 4(b)). The hyper-parameter (λ) enables counteract overfitting by limiting the size of the weights. In Fig. 4(b), the values of R^2 in terms of pressure and flow rate fluctuate as the lambda increases. The pressure prediction achieves the best performance when λ equals 0.4 and meanwhile, the highest coefficient is 0.993. On the other hand, we acquired an excellent prediction of the flow rate ($R^2 = 0.995$) as we adjusted the value of λ to 0.2. Consequently, we constructed the models based on these two values to estimate the output of EHD pumps and compared them with the experimental data (Fig. 4(c)). MLP is more accurate than RR and RF in both flow and pressure predictions, especially in large flow rate and pressure, which are closer to the experimental results. The experimental and predicted output power are depicted in Fig. 4(d). In addition, compared with the previous prediction models using RR and RF, the theoretical values of the MLP method in the predictions of Case 1 and Case 11 are closer to the actual result. Therefore, the MLP model is more accurate in our study.

3.4. Comparisons and discussion

The overall performance of three machine learning algorithms is shown in Tables 1 and 2, which includes the optimized values

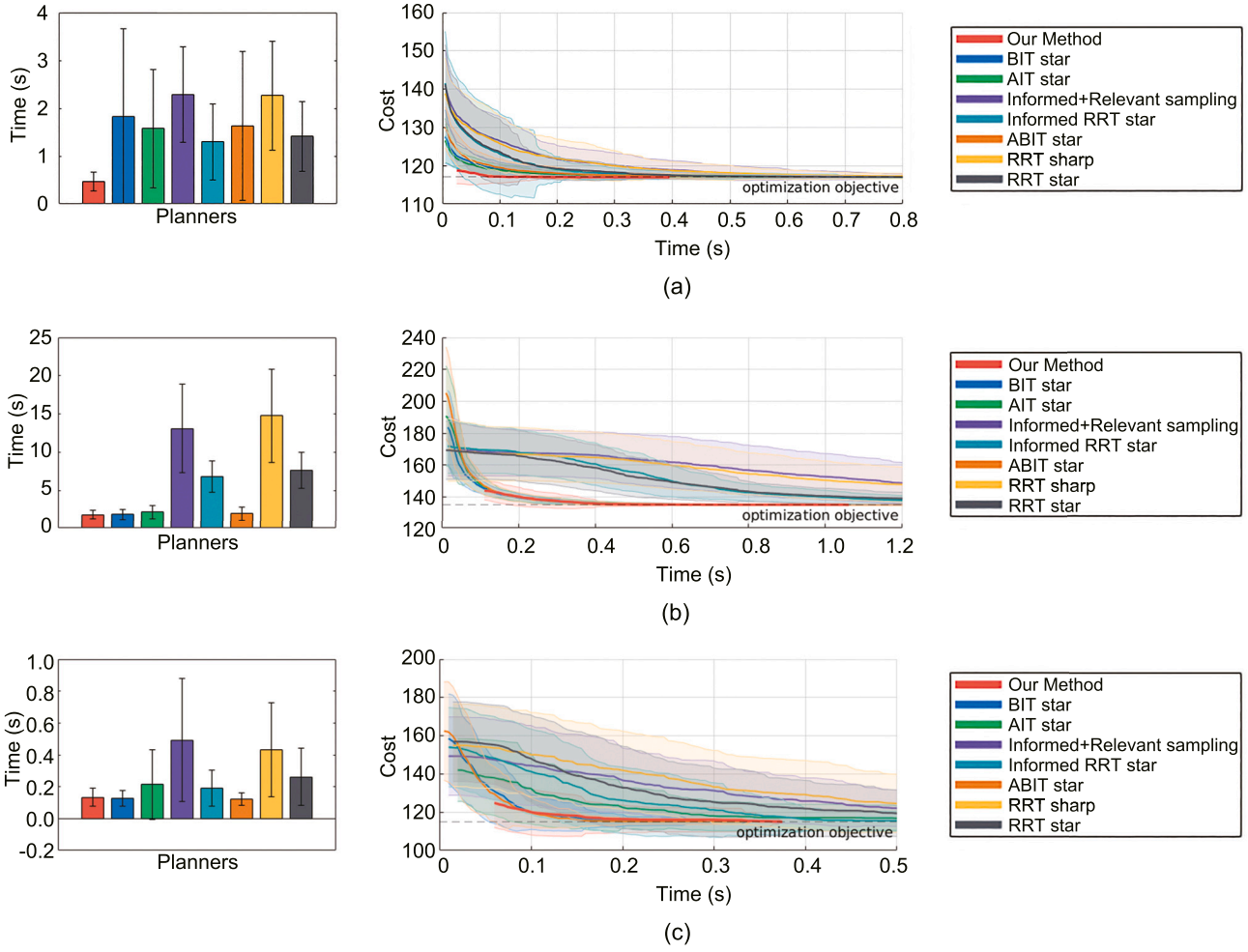

Fig. 4. (a), (b), and (c) show the 2D simulation result in 'BugTrap', the 'Maze', and the 'RandomPolygons' environments, where the left pictures are the time each planner spent to meet the optimization objective and the right pictures are the cost variations over time. Planners try to meet the optimization objective, dashed lines in the right pictures show the cost value of the optimization objective.

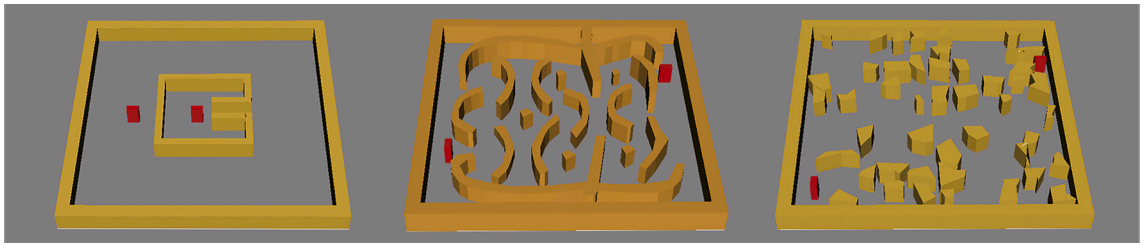

Fig. 5. The 2D simulation environments. They are the 'BugTrap', the 'Maze', and the 'RandomPolygons' in the OMPL benchmark platform, respectively. The red cuboid shows the start state and the state in the goal region.

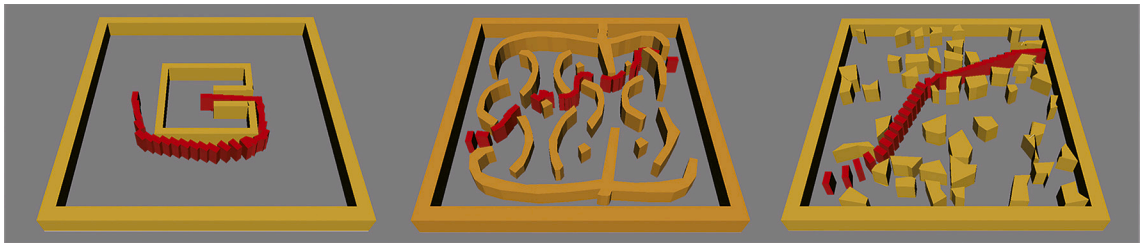

Fig. 6. The trajectories found by our planner in the 'BugTrap', the 'Maze', and the 'RandomPolygons' in the OMPL benchmark platform.

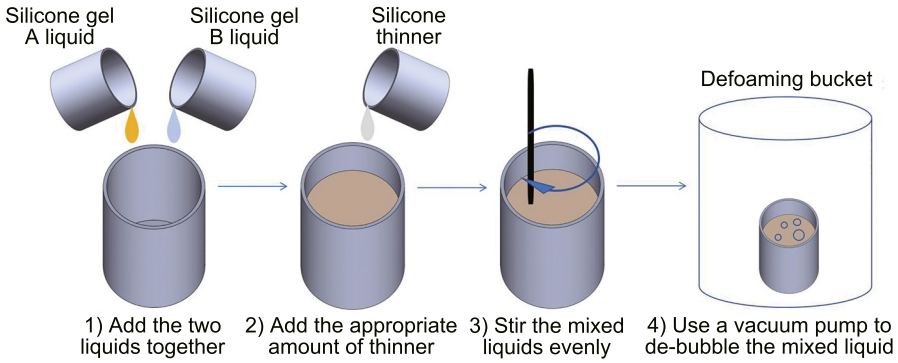

Fig. 12. Specific processes for the liquid silicone gel.

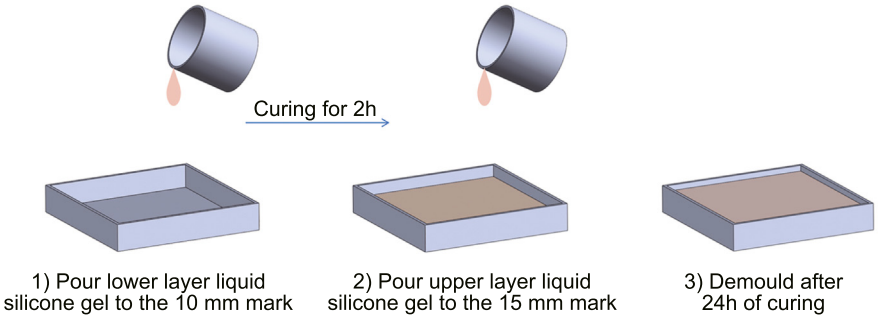

Fig. 13. Specific processes of pouring the scalp phantom.

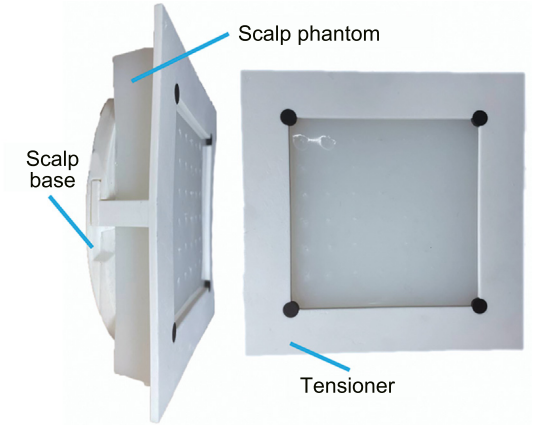

Fig. 14. The fabricated scalp phantom with the tensioner for experiments.

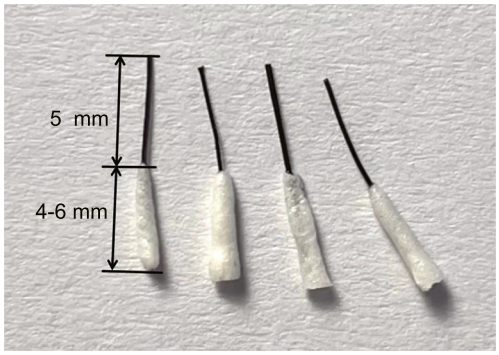

Fig. 15. Follicle units phantom. The size of the diameter of follicle part is 0.8–1.2 mm. The size of the diameter of hair is approximately 0.1 mm [20].

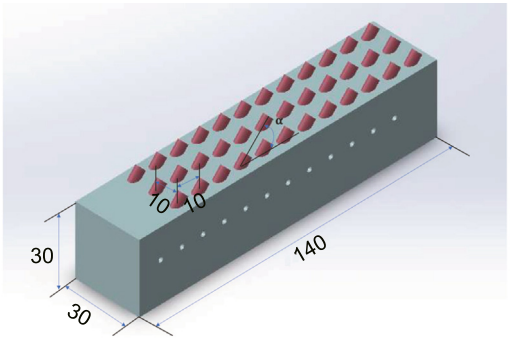

Fig. 16. The appearance and size of hair follicular chamber.

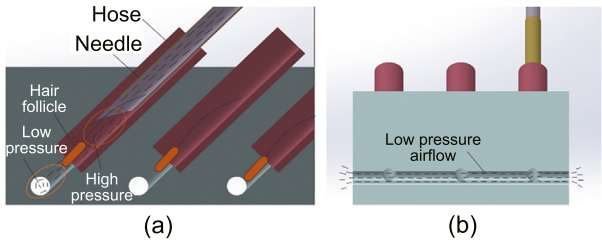

Fig. 17. Follicle chamber working principle in hair extraction process. (a) The section view of the main hole. (b) The section view of the side hole.

4.3. Experimental results

In total, three identical experiments were conducted on different scalp phantoms, and 108 sets of transplantation data were